

Performance of Cognitive Radio Sensor Networks Using Hybrid Automatic Repeat ReQuest: Stop-and-Wait

Fazlullah Khan¹ · Ateeq ur Rehman¹ · Muhammad Usman² · Zhiyuan Tan³ · Deepak Puthal²

© Springer Science+Business Media, LLC, part of Springer Nature 2018

Abstract

The enormous developments in the field of wireless communication technologies have made the unlicensed spectrum bands crowded, resulting uncontrolled interference to the traditional wireless network applications. On the other hand, licensed spectrum bands are almost completely allocated to the licensed users also known as Primary users (PUs). This dilemma became a blackhole for the upcoming innovative wireless network applications. To mitigate this problem, the cognitive radio (CR) concept emerges as a promising solution for reducing the spectrum scarcity issue. The CR network is a low cost solution for efficient utilization of the spectrum by allowing secondary users (SUs) to exploit the unoccupied licensed spectrum. In this paper, we model the PU’s utilization activity by a two-state Discrete-Time-Markov Chain (DTMC) (i.e., Free and busy states), for identifying the temporarily unoccupied spectrum bands,. Furthermore, we propose a Cognitive Radio Sense-and-Wait assisted HARQ scheme, which enables the Cluster Head (CH) to perform sensing operation for the sake of determining the PU’s activity. Once the channel is found in free state, the CH advertise control signals to the member nodes for data transmission relying on Stop-and-Wait Hybrid- Automatic Repeat-Request (SW-HARQ). By contrast, when the channel is occupied by the PU, the CH waits and start sensing again. Additionally, the proposed CRSW assisted HARQ scheme is analytical modeled, based on which the closed-form expressions are derived both for average block delay and throughput. Finally, the correctness of the closed-form expressions are confirmed by the simulation results. It is also clear from the performance results that the level of PU utilization and the reliability of the PU channel have great influence on the delay and throughput of CRSW assisted HARQ model.

Keywords Primary user detection modeling · Cognitive radio sensor networks · Wireless sensor networks · SW-HARQ · CRSW assisted HARQ model

✉ Fazlullah Khan
 fazlullah@awkum.edu.pk

Ateeq ur Rehman
 ateeq@awkum.edu.pk

Muhammad Usman
 muhammad.usman@uts.edu.au

Zhiyuan Tan
 Z.Tan@napier.ac.uk

Deepak Puthal
 Deepak.Puthal@uts.edu.au

¹ Department of Computer Science, Abdul Wali Khan University Mardan, Mardan, KPK, Pakistan

² Faculty of Engineering and Information Technology, University of Technology Sydney, Ultimo, Australia

³ School of Computing, Edinburgh Napier University, Edinburgh, UK

1 Introduction

The 21st century has witnessed exponential growth in innovative wireless applications. These applications have fulfilled the demand of users. However, they have dramatically increased the tele-traffic as well as the usage of electromagnetic spectrum, particularly the sub – 2 GHz frequency bands [1]. The expansion in wireless services leads to the dilemma of spectrum scarcity. To solve the spectrum shortage issue, spectrum regulatory bodies such as Federal Communication Commission (FCC) of the United States (US) and the European Telecommunications Standards Institute (ETSI), have investigated the spectrum utilization in various countries at different time intervals [2–7]. These studies revealed that the electromagnetic spectrum is not physically limited but improperly allocated. The inappropriate

Q1

Q2

0

1

2

3

4

5

6

7

8

9

10

11

12

13

14

15 allocation is due to the static allocation policy, using which
16 the spectrum band is exclusively assigned to the licensed
17 users, also known as primary users (PUs). The PUs are those
18 users who pay for the license and are only authorised to
19 use the assigned spectrum band. For example, the TV sta-
20 tions and cellular users are considered as PUs. The studies
21 of [2–5] have demonstrated that 15–85% of the licensed
22 spectrum are underutilized due to the current static spec-
23 trum allocation policy, resulting in spectrum scarcity. To
24 overcome this dilemma, the concept of dynamic spectrum
25 allocation (DSA) has been proposed which allows the unli-
26 censed users to find the free spectrum, access it and use
27 for data transmission without influencing the legal rights of
28 PUs [2, 8–10]. This technique leads to the emergence of
29 cognitive radio (CR) concept, which is widely accepted for
30 solving spectrum scarcity problems.

31 The term cognitive radio was first coined by Joseph
32 Mitola in 1999 [11], to solve the problem of spectrum
33 scarcity by efficient utilization of the licensed spectrum.
34 According to [12], the CR as a context-aware intelligent
35 radio has the ability to learn from the environment and
36 dynamically re-configure its transceiver, according to the
37 communication environment. Using these capabilities, the
38 CUs sense the licensed spectrum and transmit their data
39 only when the spectrum band is free from PUs. However,
40 each CU has to vacate the licensed spectrum band upon a
41 PU arrival. The CR concept has been elaborated in [13–
42 16]. These capabilities encouraged the regulatory bodies to
43 officially allow the CR concept for maximising spectrum
44 exploitation. In this regard, the phenomenon of CR has
45 been widely adopted by various wireless standards like
46 IEEE 802.11y, 802.16h, 802.22 and 1900, which has been
47 thoroughly studied in [17].

48 In literature, various aspects of CR such as working
49 cycles, designing architecture, spectrum sensing, spectrum
50 sharing, spectrum management, cooperative sensing etc [14,
51 15, 18–21] have widely been studied. However, limited
52 studies have been conducted in the direction of reliable data
53 transmission. In contrast to conventional wireless systems,
54 in CR systems, the reliability of data transmission is not
55 merely dependant on channel quality but also upon the
56 activity pattern of PUs. Hence, it is highly important to
57 accurately model the PU activity on the channel [22–
58 24]. There are numerous work performed on PU and
59 channel modeling. In our previous studies [25–29], we
60 have modelled the activities of PU over the channel using
61 discrete-time-Markov chain (DTMC), in which each state
62 represents the status of a channel. For instance, when the
63 channel is deemed to be free from PUs, it is assumed to be
64 free for CR and vice versa. Following our previous work, in
65 this paper, we also modelled the PU's channel by two-state
66 Markov chain having *free* and *busy* states. To be precise,
67 *busy* state depicts that the channel is occupied by the PU

while *free* state represents the scenario in which the channel
is free from PU and the CR uses it for data transmission.

Secondly, the CR systems face challenges similar to
conventional wireless systems, such as noise, interference,
fading etc [30, 31]. Apart from these challenges, the
CR systems have to face the dynamic activities of PUs,
resulting in more complex CR systems. In this regard,
HARQ schemes remained a favourable choice for designing
a reliable data transmission scheme. For instance, the
authors in [32] studied the performance of HARQ in
a third generation partnership project (3GPP) long term
evolution (LTE) specification over OFDMA system. D.
Nguyen et al. [33] introduced the idea of allowing a
transmitter to combine and retransmits the lost packets in
such a way that the receiver recovers the packets from a
single received copy. Ngo and Hanzo [34] surveyed the
HARQ techniques in the context of cooperative wireless
communication and a novel relay-switching technique was
proposed for enhancing the system's throughput. The
HARQ-based techniques are standardized by IEEE, for
example, 802.20, 802.16m and 802.16.1 [35–37].

Paucity of studies have take place in the direction of
achieving a reliable data transmission in CR systems. For
instance, the studies in [38–50] have assumed a reliable
data transmission without considering the dynamic activity
of the PU and its impact on the CR systems. In this regard,
in our previous studies [25–29], we have incorporated
various HARQ techniques in CR systems, assuming only
a transmitter and a receiver. In contrast to our previous
studies, in this paper, we considered an *ad hoc* CR-based
sensor network, comprises of a cluster head (CH) and
member nodes. The CH performs sensing and once it deems
a free time-slot (TS), it initiates and broadcasts a clear-
to-send (CTS) signal to the member nodes and waits for
the response. The member nodes respond with a join-
request and the CH selects the member node for data
transmission, based on first-come-first-serve principle. The
selected member node then starts transmitting its data, using
a stop-and-wait HARQ approach. On the other hand, when
the channel is found to be in *busy* state, the CH remains
silent and starts sensing again in the subsequent TS. This
process continues until a free TS is found.

This paper mainly focuses on the efficient utilization of
licensed spectrum by allowing CR-based member nodes to
use a PU channel, which results in a higher throughput and
a lower delay. We have proposed a CRSW-assisted HARQ
model for solving the problem of inefficient utilization of
the spectrum. The main contributions of this paper are as
follow.

- Designing and modeling a CR-based *ad hoc* network,
assisted by a HARQ scheme for the sake of introducing
the cognitive capabilities with the conventional SW-HARQ

120 scheme and apply it to sensor network to attain a
 121 reliable data delivery.
 122 – The CRSW-assisted HARQ model is analytically
 123 modelled using a probabilistic based approach, using
 124 which closed-form expressions for *average packet*
 125 *delay* and *throughput* are derived.
 126 – Theoretical results of CRSW-assisted HARQ model
 127 are validated through simulations using MATLAB.
 128 Moreover, the probability distribution, based on *end-to-*
 129 *end packet delay*, is investigated through Monte Carlo
 130 simulations.

131 The remaining paper is organized as follows. In
 132 Section 2, the system model is elaborated, with primary user
 133 system and assumptions in Section 2.1, whereas Section 2.2
 134 describes modeling of cognitive radio sensor networks. The
 135 cognitive radio sense and wait assisted HARQ is discussed
 136 in Section 2.3, operation of a cluster head in Section 2.4,
 137 and operation of a sensor node in Section 2.5. Analysis of
 138 the CRSW assisted HARQ model is discussed in Section 3,
 139 delay analysis is performed in Section 3.1, and throughput
 140 analysis in Section 3.2, followed by results and discussion
 141 in Section 4. Finally, Section 5 elaborates future research
 142 scope and concludes the paper.

143 **2 System model**

144 In this section, we consider step-by-step description of the
 145 system model and assumptions.

146 **2.1 Primary user system and assumptions**

147 In this paper, we consider a wireless channel which is
 148 exclusively allocated to the PU. For simplicity, we assume
 149 the channel is divided into equal length time slots (TS),
 150 where each has a duration of T seconds, as illustrated in
 151 Fig. 1. In our proposed model, the PU is synchronized
 152 to access the channel, based on the TSs. Hence, PUS
 153 transmission resemble with the starting and ending of a TS.
 154 For example, as depicted in Fig. 1, if a TS is sensed and the
 155 activity of the PU is deemed, then PU remains active until
 156 the end of TS. However, if a TS is found unoccupied by the
 157 PU, then TS remains unoccupied till the end of its duration.
 158 With the help of the above procedure, the PU's transmission
 159 always occur in the integer multiple of TSs, which means
 160 the transmission is always equal to 1, 2, 3, ... but not in
 161 floating points.

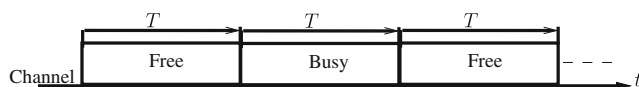


Fig. 1 TS of equal length, Busy or Free period

Moreover, preserving the legal rights of the PU, it can
 utilize any TS independently with the same probability.
 Hence, based on these assumptions, the activity of PU
 over a wireless channel may be modeled by a Discrete-
 Time Markov Chain (DTMC) having two states (free, busy),
 where the state to state traversing probabilities are depicted
 in Fig. 2. Specifically, the 'free' state symbolizes that the PU
 is inactive, whereas, the 'busy' state shows that the channel
 is occupied by the PU at the respective TS.

Following the properties of DTMC, a TS could be
 in any state at time t , i.e., $S(t) \in \{free(t), busy(t -$
 $1), \dots busy(1)\}$. In other words, it can be expressed as

$$S = \{S_1, S_2\}. \tag{1}$$

where state S_1 represents a free TS and state S_2 denotes
 a busy TS. To determine the state of the TS at time t , we
 have the condition probability that the TS was in state S_j
 at TS $(t + 1)$, given that it was in S_i in TS t , which can be
 mathematically formulated as

$$P_{i,j} = \{S(t + 1) = S_j | S(t) = S_i, \dots, S(1) = S_1\},$$

$$= \{S(t + 1) = S_j | S(t) = S_i\}, \text{ where}$$

$$i = 1, 2, j = 1, 2 \text{ and } t = 1, 2, \dots \tag{2}$$

Moreover, based on the principles of DTMC, each state
 must have a probability less than 1 (i.e., $0 \leq P_{i,j} \leq 1$) and
 the outgoing transitions probabilities from state S_i should be
 equal to one $\sum_{j \in S} P(i, j) = 1$ [52]. Hence, in our proposed
 model, we have

$$P_{1,1} + P_{1,2} = 1, \text{ and } P_{2,2} + P_{2,1} = 1. \tag{3}$$

The state-to-state transition matrix of two states DTMC is
 represented by \mathbf{P} and expressed as,

$$\mathbf{P} = \begin{bmatrix} P_{1,1} & P_{1,2} \\ P_{2,1} & P_{2,2} \end{bmatrix}. \tag{4}$$

where $P_{1,1}$ and $P_{2,2}$ represent the probability of being in
 same state whereas $P_{1,2}$ and $P_{2,1}$ denotes the traversing
 of states, i.e., from free to busy state and from busy to

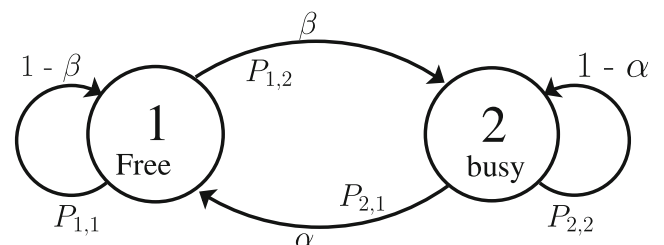


Fig. 2 Two-state DTMC model of the PU system, where α and β represents the transition from busy to free and from free to busy state, respectively [26, 51]

190 free state, respectively, as shown in Fig. 2. Then, when the
 191 Markov chain become steady i.e.,

$$\mathbf{p}(t + 1) = \mathbf{P}^T \mathbf{p}(t), \quad (\mathbf{P}^T)^t \mathbf{p}(1). \quad (5)$$

192 where $\mathbf{p}(1)$ represents the starting state (i.e., $\mathbf{p}(1) = [1, 0]$).
 193 Furthermore, \mathbf{P}^T is a left stochastic matrix due to the fact
 194 that summation of each column is equal to 1 [53], which
 195 is also verified in Eq. 3. Hence, when the Markov chain
 196 becomes steady, we have,

$$\mathbf{p}(t + 1) = \mathbf{p}(t). \quad (6)$$

197 Moreover, let us symbolize the steady state probabilities
 198 by $\boldsymbol{\pi} = [\pi_1, \pi_2]$, then we have a recursive equation of [52]

$$\boldsymbol{\pi} = \mathbf{P}^T \boldsymbol{\pi}. \quad (7)$$

199 In Eq. 7, $\boldsymbol{\pi}$ is the right Eigen vector of the transition metric
 200 \mathbf{P} with the Eigen value of 1. It is important to note that the
 201 steady state vector satisfies the condition of

$$\pi_1 + \pi_2 = 1 \quad \text{or} \quad \boldsymbol{\pi}^T \mathbf{1} = 1. \quad (8)$$

202 where $\mathbf{1}$ represents a column vector having all 1 values. For
 203 the sake of deriving close-form expressions for both states,
 204 let P_f and P_b represent the probability of being in the free
 205 state and busy state, then we have,

$$P_b \alpha = P_f \beta. \quad (9)$$

which reaches to:

$$\pi_1 = \left(\frac{P_{2,1}}{P_{1,2} + P_{2,1}} \right) \quad \text{and} \quad \pi_2 = \left(\frac{P_{1,2}}{P_{1,2} + P_{2,1}} \right). \quad (10)$$

which can also be represented by:

$$P_f = \frac{\alpha}{\alpha + \beta} \quad \text{and} \quad P_b = \frac{\beta}{\alpha + \beta} \quad (11)$$

208 Following the above discussion, we may conclude that
 209 when a TS is not occupied by the PU, it will remain
 210 free for the whole T seconds duration. Thus, for the sake
 211 of improving the overall channel utilization, the SU may
 212 access the free TSs and transmits its own data packets [9,
 213 54]. In the following subsection, we will discuss in detail
 214 the procedure of finding a free TS and data transmission.

2.2 Modeling the cognitive radio sensor network (CRSN)

217 We assume that a CRSN is employed in an area of a
 218 PU system, where signal-to-noise ratio is very high. A
 219 sensor network has low power, low processing capability,
 220 and exposed to noise, so these networks cannot perform
 221 well in the presence of high noise and interference in
 222 the unlicensed band. In this paper, CRSN consists of one

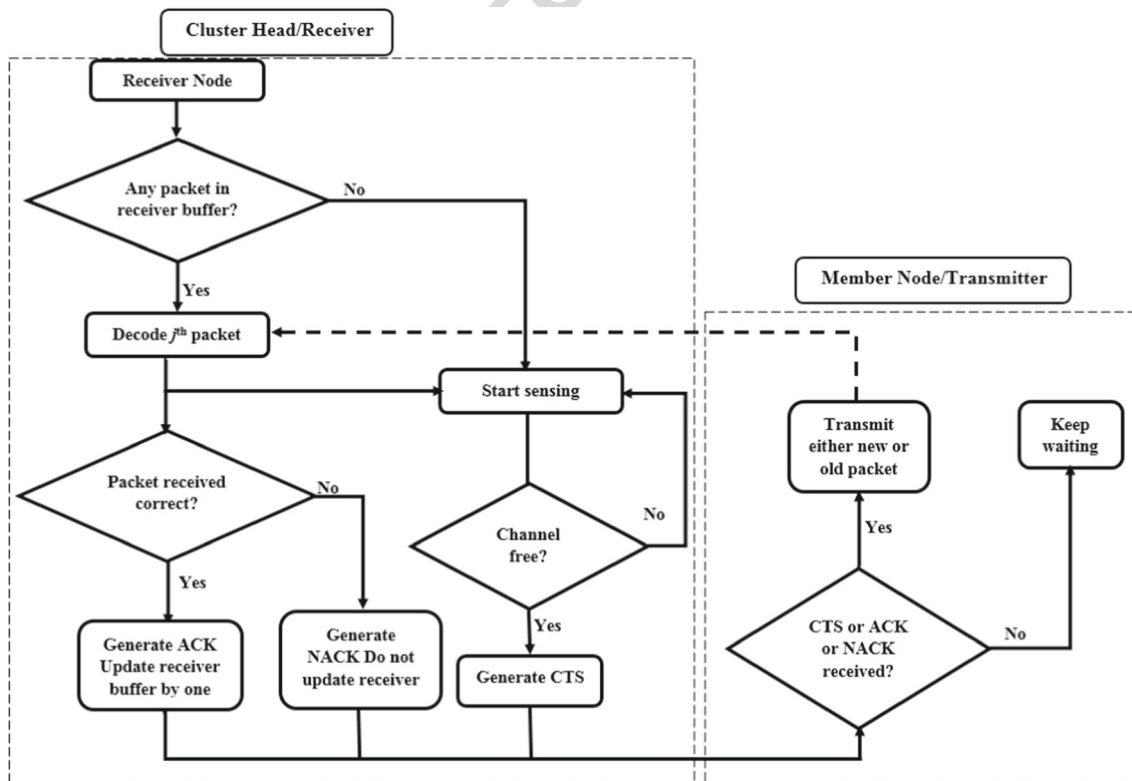


Fig. 3 Flow chart of CRSW assisted HARQ model

223 cluster comprise of Cluster Head (CH) and member nodes.
 224 The CH communicates with member nodes, where the
 225 member nodes use time division multiple access mechanism
 226 for transmitting data packets in a specified time-frame.
 227 Specifically, the CH perform sensing in order to ideally
 228 detect the activity (free/busy) of the PU over the channel,
 229 regardless of false-alarm and miss-detection. Hence, when
 230 a free TS is detected, a member node transmits a packet to
 231 the CH. On the other hand, when CH detects a busy TS,
 232 then it waits until a free TS is deemed. The member nodes
 233 follows the stop and wait hybrid automatic repeat request
 234 (SW-HARQ) approach for data transmission, which will be
 235 explained in the following sections.

236 **2.3 Cognitive radio sense and wait (CRSW) assisted**
 237 **HARQ**

238 The proposed CRSN perform two vital functions of sensing
 239 PU channel and data transmission. For instance, when a
 240 free TS is deemed, then the member node uses the classic
 241 SW-HARQ approach for the sake of reliably transmitting
 242 data packet to the CH. To achieve high reliability, the
 243 CH incorporates Reed-Solomon (RS) encoding/decoding
 244 technique, in order to detect and/or rectify errors in the
 245 received packet. To do so, we assume that each data packet
 246 is encoded with RS codeword $RS(N_d, K_d)$ [55], where K_d
 247 is number of information and N_d is coded symbol. The
 248 propagation time of each coded packet from member node
 249 to the CH is T_r seconds, where $T_r < T$. The RS code
 250 is assumed to be capable of perfectly detecting errors as
 251 well as rectifies $e = \frac{N_d - K_d}{2}$ error symbols. Hence, when
 252 a received packet has more than e errors, it is considered
 253 as erroneous which requires retransmission. The round-trip-
 254 time of a packet is T seconds, which can be defined as, the
 255 time duration from the transmission until the reception of its
 256 feedback.

257 Based on the above assumptions, the data is exchanged
 258 between member nodes and CH over PU channel using
 259 the principal of CRSW assisted HARQ model depicted in
 260 Fig. 3, and explained in Algorithm 1. The detail operations
 261 of CH and member nodes are provided below.

262 **2.4 Operations of cluster head**

263 In our proposed model, the CH performs the following
 264 operations. First, it performs sensing operation for the sake
 265 of detecting the activity of a PU over the channel. Once it
 266 detects the activity of a PU, it will wait for a while and then
 267 starts sensing again. This process continues until a free TS is
 268 found. Secondly, we assume that the CH has a finite buffer
 269 for storing the index number of packets that is expected
 270 to be received. The buffer follows First-in-First-out (FIFO)
 271 principle. Thirdly, when a free TS is detected, the CH

broadcasts an Clear-to-Send (CTS) signal to the member 272
 nodes and waits for them to respond. We assume that the 273
 CH selects a member node for transmission based on the 274
 First-Come-First-Serve (FCFS) principle. In other words, 275
 it means that the member node which receives the CTS 276
 signal and respond earlier is allowed to transmit new/old 277
 packet. It is worth mentioning that each member node 278
 acknowledges the CTS signal with a join-request (Ready- 279
 to-Send) response. When the corresponding member node 280
 finishes its transmission, it then starts waiting for the 281
 reception of feedback signal from the CH, which will be 282
 explained in the following subsection. 283
 284

Algorithm 1 CRSW assisted HARQ Algorithm

Initialization: N_p = number of packets, $T_d = N$, $T_s = m$, j
 = 1, TS = 1

Input: T_d, T_s , packets

```

1: procedure
2:   while  $i \leq N_p$  do
3:     if CH has any packet in buffer then
4:       decode the packet and start sensing a TS
5:     else
6:       CH senses a TS
7:     if a TS is detected idle then
8:       broadcast a CTS to member nodes
9:     if CTS/ACK/NACK received by sensor nodes then
10:      (re)transmit a packet
11:     if the  $j$ th packet is correctly received then
12:       CH sends ACK
13:        $j = j + 1$ 
14:     elseif the  $j$ th packet is erroneous then
15:       CH sends NACK
16:       Goto line 9
17:     end if
18:     end if
19:     else
20:       Wait for CTS
21:     end if
22:      $TS = TS + 1$ 
23:     end if
24:     end if
25:   end while
26: end procedure
    
```

On the other side, when CH receives a complete RS 286
 coded packet, it performs decoding/correction process in 287
 order to generate positive acknowledgment (ACK) or 288
 negative acknowledgment (NACK) signal for an error-free 289
 or erroneous packet respectively. Specifically, when an 290
 error-free packet is received, the CH increments its buffer 291
 index by one and generates immediately an ACK signal and 292

293 transmits to the respective member node. In contrast, when
 294 an erroneous packet is received, the buffer index remains
 295 unchanged and the CH responds back with a NACK signal
 296 to the member node. This process continues until all packets
 297 are correctly received.

298 **2.5 Operation of member node**

299 The member nodes of a CH has a joint buffer in which all
 300 the packets are stored in an ascending order. Each member
 301 node transmits only one packet at a time from this buffer
 302 due to the implementation of SW-HARQ approach. Once a
 303 member node receives CTS signal and the CH authorizes
 304 it for packet transmission, it then transmits either new/old
 305 packet waiting in the joint buffer. At this time interval,
 306 the rest of the member nodes are assumed to remain silent
 307 (even if they have responded with an RTS signal) until
 308 the advertisement of another CTS signal and this concept
 309 is out of the scope of this paper. Furthermore, after the
 310 transmission of the i th packet, the corresponding member
 311 node waits for T_w seconds to receive the feedback of the
 312 transmitted packet. Hence, when an ACK is received, the
 313 member node deletes the copy of the successfully received
 314 packet from the joint buffer and increments its sequence by
 315 one. On the other hand, when a NACK signal is received,
 316 the corresponding packet remains in the joint buffer with
 317 the same index number. Note that the erroneous packet
 318 will be retransmitted again by any member node in the
 319 next free TS. This process continues until all the packets
 320 are correctly transmitted from the member nodes joint
 321 buffer.

322 **3 Analysis of CRSW assisted HARQ model**

323 In this section, we analyze CRSW assisted HARQ model
 324 both in terms of two performance metrics 1) the average
 325 block delay and 2) the Average throughput.

326 **3.1 Average block delay (T_D)**

327 The average block delay can be defined as the average num-
 328 ber of TSs or T_r 's required for the error-free transmission of
 329 a packet. In contrast to conventional transmission schemes,
 330 in our proposed model, the delay is not only imposed by
 331 channel errors, but also comprise of the delay introduced
 332 the unavailability of the PU channel for CR transmission.
 333 Therefore, let D_P represents the delay caused by the uti-
 334 lization the channel by PU and D_e is the delay induced by
 335 one or more retransmissions of a packet. In order to analyze
 336 the total delay T_D of the proposed CRSW assisted HARQ
 337 system, we will first investigate the delay induce by the PU
 338 activity.

Based on the probability, P_b of the PU system defined in 339
 Eq. 11, the average delay D_P for a CH to detect a free TS 340
 can be calculated as 341

$$\begin{aligned} D_P &= E[D_P(i)] \\ &= E[(i - 1)T] \\ &= \sum_{i=1}^{\infty} (i - 1)T P_b^{i-1} (1 - P_b) \\ &= \frac{P_b T}{1 - P_b} \end{aligned} \tag{12}$$

where $D_P(i)$ represents the delay for detecting an i th 342
 free TS which can be used by the member node for data 343
 transmission, while the prior $(i - 1)$ TS were occupied by PU 344
 which causes a delay of $(i-1)T$. Upon substituting $P_b = \frac{\beta}{\alpha + \beta}$ 345
 presented in Eq. 11 into Eq. 12, we reach to the following 346
 closed-form expression 347

$$T_{DP} = \frac{\beta T}{\alpha} \tag{13}$$

Secondly, when an i th free TS is detected by the CH, it 348
 requests the member node for the transmission of a packet 349
 which is explained in Sections 2.4 and 2.5. The authorized 350
 member node transmit a packet to the CH, however, due 351
 to communication impairments, there is a possibility that 352
 the packet might be received erroneously, which requires 353
 retransmission. The retransmission process continues until 354
 the corresponding packet is received without errors. Hence, 355
 to accommodate the case of one or more transmissions of a 356
 single packet, let us assume that probability of packet being 357
 in error is P_e , then have 358

$$\begin{aligned} D_e &= \sum_{i=1}^{\infty} (i) P_e^{i-1} (1 - P_e) \\ &= \frac{1}{1 - P_e} \end{aligned} \tag{14}$$

Now the total block delay can be achieved as 359

$$\begin{aligned} T_D &= (D_P + T) \times D_e, \\ &= \left(\frac{\beta T}{\alpha} + T \right) \times \frac{1}{1 - P_e}, \\ &= \left(\frac{\alpha + \beta}{\alpha} \right) \times \frac{T}{1 - P_e} \text{ (seconds)}. \end{aligned} \tag{15}$$

Moreover, the normalized T_D in terms of packet transmis- 360
 sion (T_r) can be expressed as 361

$$T_D = \left(\frac{\alpha + \beta}{\alpha} \right) \times \frac{1}{1 - P_e} \times \frac{T_r + T_w}{T_r} (T_r's). \tag{16}$$

From Eqs. 15 and 16, we may conceive that the block delay 362
 increases with increase in the utilization level of the PU, 363
 decrease in the channel quality and with the increase in the 364
 waiting time spend for the reception of feedback. 365

366 **3.2 Average throughput**

The throughput of the proposed CRSW assisted HARQ 367
 model can be defined as the successful transmission rate 368

369 of a packet in TS. The successful transmission of packets
 370 depends on the successful detection of free TS by a CH and
 371 error-free transmission of packet to the CH. To investigate
 372 throughput of the proposed system, let us represent the
 373 probability of successfully delivering a packet to CH by
 374 $P_S(i)$ in i th TS, while the remaining $(i - 1)$ TSs were either
 375 occupied by PU or packet was received in error. Then, $P_S(i)$
 376 can be calculated as shown in Eq. 17 below,

$$P_S(i) = \sum_{j=1}^i P_f(j|i)P_S(j|i), \quad (17)$$

377 where the probability that PU channel is free in j/i TS is
 378 represented by $P_f(j|i)$, while $P_S(j|i)$ is the probability that
 379 the member node successfully transmits a packet in j TS.
 380 Therefore, we can write Eq. 18 based on Eq. 17 as follow,

$$\begin{aligned} P_S(i) &= \sum_{j=1}^i \binom{i}{j} P_f^j P_b^{(i-j)} P_e^{(j-1)} (1 - P_e), \\ &= \sum_{j=1}^i \binom{i}{j} \left(\frac{\alpha}{\alpha+\beta}\right)^j \left(\frac{\beta}{\alpha+\beta}\right)^{(i-j)} P_e^{(j-1)} (1 - P_e). \end{aligned} \quad (18)$$

381 Based on the above equation, we can readily obtain the
 382 normalized throughput as:

$$\begin{aligned} \eta &= \sum_{i=1}^{\infty} \frac{1}{i} \times P_S(i), \\ &= \left[\sum_{i=1}^{\infty} \sum_{j=1}^i \binom{i}{j} \left(\frac{\alpha}{\alpha+\beta}\right)^j \left(\frac{\beta}{\alpha+\beta}\right)^{(i-j)} \times P_e^{(j-1)} \times \right. \\ &\quad \left. \times (1 - P_e) \right] \text{ (packets per TS)}. \end{aligned} \quad (19)$$

383 Moreover, the normalized throughput in terms of
 384 packets per T_r can be expressed as

$$\bar{\eta} = \frac{T_r}{T} \times \eta = \frac{T_r}{T_r + T_w} \times \eta \text{ (packets per } T_r). \quad (20)$$

385 4 Performance results

386 In this section, we evaluate both the delay and throughput
 387 performance of the proposed CRSW assisted HARQ
 388 scheme in terms of PU channel utilization and channel
 389 reliability. We illustrate the effect of packet error probability
 390 (P_e) and the probability of a channel being in busy state
 391 (P_b) on the performance of the proposed scheme. The
 392 CRSW assisted HARQ mode has been build with the
 393 help MATLAB, where sixty thousands packets have been
 394 transferred for each scenario. The simulation start from the
 395 sensing of the first TS and ends on the successful reception
 396 of total N_s packets.

397 Figure 4 depicts the throughput achieved by CRSW
 398 assisted HARQ model against P_e and P_b of the channel.

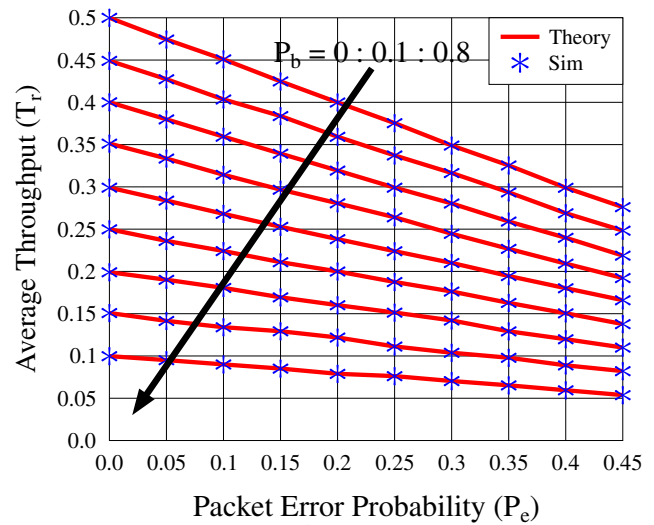


Fig. 4 Throughput versus packet error probability P_e for the CRSW assisted HARQ model related with different P_b , when presuming $T_r = 1$ and $T_w = 1$ seconds. Average throughput performance is examined for different values of P_e , where results are calculated in terms of T_r

The formula used for calculating the throughput is given in Eq. 21 as

$$\eta'_S = \frac{N_s}{N_{ts}} \cdot \frac{T_r}{T_r + T_w} \text{ (packets per } T_r), \quad (21)$$

where N_s is the sum of packets correctly transmitted by the member nodes in the total N_{ts} TSs.

We can see in Fig. 4 that the throughput is at its peak for $P_e = 0$, this means that the channel is highly reliable and therefore, the rate of retransmission is minimum. However, as shown in Fig. 4, the throughput drops when P_e increases. This is because, the channel reliability reduces which results in low throughput. The decrease in throughput is almost linear, this is due retransmission of packets. For certain P_e , the throughput reaches to its maximum level, when there is no PU activity on the channel, i.e. when $P_b = 0$. But when, P_b increases, the achievable throughput considerably decreases, as the CH has to wait longer duration for detecting free TSs. For instance, both when P_e and P_b are zero, then the throughput is at its maximum with the value of .5 seconds. This means that the channel is always free from PU and packet transmission is always successful in the first TS. Furthermore, it is pretty clear form Fig. 4 that the analytical results calculated from Eq. 20 agree well with our simulation results.

After investigating the throughput performance, we now explain on the delay of the CRSW assisted HARQ model. First we study average block delay, as presented in Fig. 5. It is worth mentioning here that for simulation results, we have calculated the average packet delay using Eq. 22

$$T_{DS} = \frac{N_{ts} \cdot (T_r + T_w)}{N_s} \text{ (seconds)}. \quad (22)$$

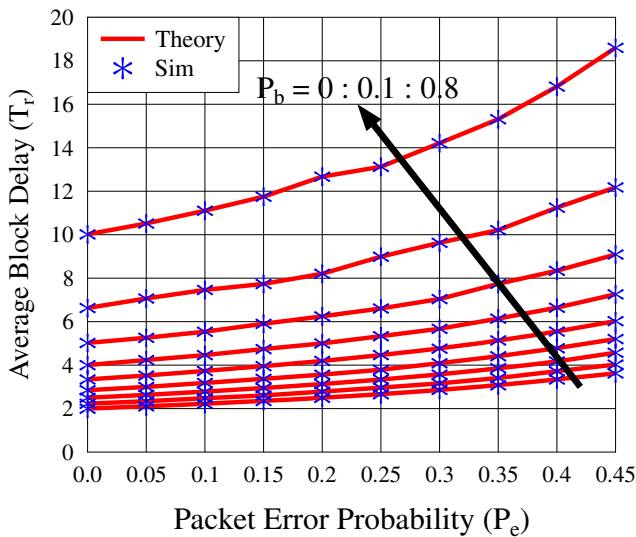


Fig. 5 Average block delay of the CRSW assisted HARQ model against probability of packet error for different P_b values

where N_s is the sum of packets correctly transmitted by member nodes in the total number of TSs N_{ts} . The results shown in Fig. 5 are normalized by T_r , producing Eq. 23

$$T'_{DS} = \frac{T_{DS}}{T_r} (T_r s). \quad (23)$$

Figure 5, depicts the average packet delay of the CRSW assisted HARQ model. For certain P_b , the average packet delay reaches to a minimum level, particularly when the channel is reliable, i.e. when $P_e = 0$. But when, P_b and/or P_e increases, the average packet delay considerably

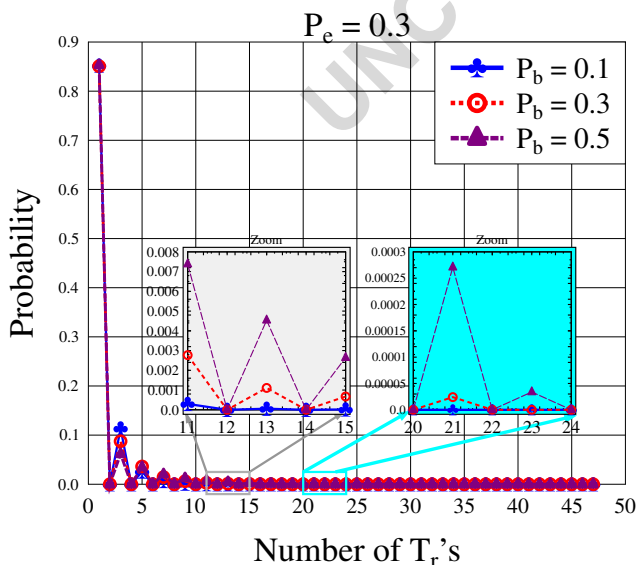


Fig. 6 Characterizing the probability distribution of the E2E packet delay for $P_b = \{0.1, 0.3, 0.5\}$ and $P_e = \{0.3\}$

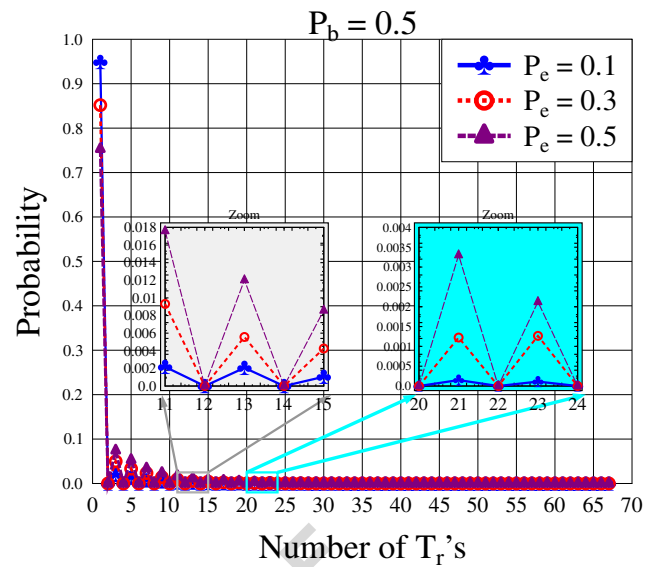


Fig. 7 Investigation of probability distribution of the E2E packet delay for $P_e = \{0.1, 0.3, 0.5\}$ when $P_b = \{0.5\}$

increases. This increase in average packet delay is due to the fact that the high value P_e causes more retransmissions while increase in P_b value decreases the chances of transmission for a member node. Furthermore, it is pretty clear from Fig. 5 that the analytical results calculated from Eq. 16 agree well with our simulation results.

In Fig. 6, we illustrate the end-to-end (E2E) packet delay of the CRSW assisted HARQ model. In our simulations, the E2E delay is defined as the time taken by a packet from its first transmission attempt to its final successful reception divided by total total number of packet.

For E2E, we consider a vector \mathbf{v} having length of N_s for storing E2E delay of each transmitted packet; then let $\mathbf{v}(i)$ denotes the E2E delay of the i th packet, then the probability distribution (P_d) of E2E packet delay shown in Fig. 6 may be calculated as:

$$P_d = \frac{\sum_{i=1}^{N_s} \delta(\mathbf{v}(i) - n)}{N_s}, \quad 1 \leq n \leq \max(\mathbf{v}). \quad (24)$$

where δ function is used for finding the number of TS took by each packet. For example, if 100 packets are successfully received in their first transmission attempt in and 80 packets have taken two T_r 's then the distribution becomes $P_d = [100/N_s, 80/N_s, \dots]$ (Fig. 7).

5 Conclusion

The latest trends in wireless communication technologies have given the notion that the spectrum is scarce. The spectrum scarcity is due to the static allocation of spectrum,

460 and to overcome this issue we need a perfect PU detection
 461 model. In this paper, we have proposed and examined
 462 the performance of CRSW assisted HARQ model for
 463 efficient detection the PU channel. The throughput and
 464 delay of CRSW assisted HARQ model has been analyzed
 465 mathematically and validated via simulations. Accuracy
 466 of the derived closed-form expressions of CRSW assisted
 467 HARQ model has been verified using MATLAB simulation.
 468 We conclude from simulation results that delay and
 469 throughput performances of CRSW assisted HARQ model
 470 are mainly affected by both the activities of the PU as well
 471 as by the reliability of the PU channel used by SU. When
 472 the PU channel is not free, this causes low throughput of the
 473 CRSW assisted HARQ model and higher delay, though the
 474 channel might be reliable, i.e., $P_e = 0$. In future research
 475 we aim to evaluate the performance of CRSW assisted
 476 HARQ model in a realistic imperfect sensing scenarios and
 477 multi-cluster scenarios.

478 References

- 479 1. Goldsmith A, Jafar SA, Maric I, Srinivasa S (2009) Breaking
 480 spectrum gridlock with cognitive radios: an information theoretic
 481 perspective. *Proc IEEE* 97(5):894–914
- 482 2. FCC (2002) Et docket No. 02-155 spectrum policy task force
 483 report technical report
- 484 3. Staple G, Werbach K (2004) The end of spectrum scarcity
 485 [spectrum allocation and utilization]. *IEEE Spectr* 41(3):48–52
- 486 4. Yang J (2005) Spatial channel characterization for cognitive
 487 radios, Master's Thesis, EECS Department, University of Califor-
 488 nia, Berkeley, Tech. Rep. UCB/ERL M05/8. [Online]. Available:
 489 <http://www.eecs.berkeley.edu/Pubs/TechRpts/2005/4293.html>
- 490 5. McHenry MA, Tenhula PA, McCloskey D, Roberson DA, Hood
 491 CS (2006) Chicago spectrum occupancy measurements & analysis
 492 and a long-term studies proposal. In: Proceedings of the first
 493 international workshop on technology and policy for accessing
 494 spectrum (TAPAS)
- 495 6. Cabric D (2007) Phd thesis on cognitive radios: system design
 496 perspective. University of California at Berkeley
- 497 7. Islam MH, Koh CL, Oh SW, Qing X, Lai YY, Wang C, Liang
 498 YC, Toh BE, Chin F, Tan GL, Toh W (2008) Spectrum survey
 499 in singapore: occupancy measurements and analyses. In: 3rd
 500 International conference on cognitive radio oriented wireless
 501 networks and communications (CrownCom), pp 1–7
- 502 8. Hossain E, Niyato D, Han Z (2009) Dynamic spectrum access and
 503 management in cognitive radio networks. Cambridge University Press
- 504 9. Zhao Q, Sadler BM (2007) A survey of dynamic spectrum access.
 505 *IEEE Signal Process Mag* 24(3):79–89
- 506 10. Akhtar F, Rehmani MH, Reisslein M (2016) White space:
 507 definitional perspectives and their role in exploiting spectrum
 508 opportunities. *Telecommun Policy* 40(4):319–331
- 509 11. Mitola J, Maguire GQ (1999) Cognitive radio: making software
 510 radios more personal. *IEEE Pers Commun* 6(4):13–18
- 511 12. Haykin S (2005) Cognitive radio: brain-empowered wireless
 512 communications. *IEEE J Select Areas Commun* 23(2):201–220
- 513 13. Cabric D, Mishra SM, Brodersen RW (2004) Implementation
 514 issues in spectrum sensing for cognitive radios. In: Conference
 515 on signals, systems and computers, conference record of the
 516 thirty-eighth asilomar, vol 1, pp 772–776
14. Ganesan G, Li Y (2007) Cooperative spectrum sensing in
 cognitive radio, part I: two user networks. *IEEE Trans Wirel*
 Commun 6(6):2204–2213
15. Yucek T, Arslan H (2009) A survey of spectrum sensing
 algorithms for cognitive radio applications. *IEEE Commun Surv*
 Tutor 11(1):116–130. Quarter
16. Axell E, Leus G, Larsson EG, Poor HV (2012) Spectrum sensing
 for cognitive radio: state-of-the-art and recent advances. *IEEE*
 Signal Process Mag 29(3):101–116
17. IEEE recommended practice for information technology-
 telecommunications and information exchange between systems
 wireless regional area networks (WRAN)-specific requirements-
 part 22.2: installation and deployment of IEEE 802.22 systems,"
 IEEE Std 802.22.2-2012, pp 1–44, Sept 2012
18. Akyildiz IF, Lee W-Y, Vuran MC, Mohanty S (2006) Next
 generation/dynamic spectrum access/cognitive radio wireless
 networks: a survey. *Comput Netw J (Elsevier)* 50(13):2127–2159
19. He A, Gaeddert J, Bae KK, Newman TR, Reed JH, Morales L,
 Park C-H (2009) Development of a case-based reasoning cognitive
 engine for IEEE 802.22 WRAN applications. *ACM SIGMOBILE*
 Mobile Comput Commun Rev 13(2):37–48
20. Liang YC, Zeng Y, Peh EY, Hoang AT (2008) Sensing-
 throughput tradeoff for cognitive radio networks. *IEEE Trans*
 Wirel Commun 7(4):1326–1337
21. Khan F, Nakagawa K (2013) Comparative study of spectrum
 sensing techniques in cognitive radio networks. In: World
 Congress on computer and information technology (WCCIT)
 2013, pp 1–8
22. Su H, Zhang X (2008) Cross-layer based opportunistic MAC
 protocols for QoS provisionings over cognitive radio wireless
 networks. *IEEE J Selected Areas Commun* 26(1):118–129
23. Lee W-Y, Akyildiz IF (2008) Optimal spectrum sensing
 framework for cognitive radio networks. *IEEE Trans Wirel*
 Commun 7(10):3845–3857
24. Akin S, Gursoy MC (2011) Performance analysis of cognitive
 radio systems under qos constraints and channel uncertainty. *IEEE*
 Trans Wirel Commun 10(9):2883–2895
25. Rehman AU, Thomas VA, Yang LL, Hanzo L (2016) Performance
 of cognitive selective-repeat hybrid automatic repeat request.
IEEE Access 4:9828–9846
26. Rehman AU, Dong C, Yang LL, Hanzo L (2016) Performance of
 cognitive stop-and-wait hybrid automatic repeat request in the face
 of imperfect sensing. *IEEE Access* 4:5489–5508
27. Rehman AU, Dong C, Thomas V, Yang LL, Hanzo L (2016)
 Throughput and delay analysis of cognitive go-back-n hybrid
 automatic repeat request using discrete-time markov modelling.
IEEE Access 4:9659–9680
28. Rehman AU, Yang LL, Hanzo L (2017) Delay and throughput
 analysis of cognitive go-back-n harq in the face of imperfect
 sensing. *IEEE Access* 4
29. Khan F, Rehman AU, Jan MA, Alam M (2017) Modeling
 resource allocation for real time traffic in cognitive radio
 sensor networks. In: International conference on future intelligent
 vehicular technologies, pp 1–8
30. Lin S, Costello DJ (1999) Error control coding: fundamentals and
 applications, 2nd edn. Prentice-Hall, Upper Saddle River
31. Hanzo L, Liew T, Yeap B, Tee R, Ng SX (2011) Turbo coding,
 turbo equalisation and space-time coding. EXIT-chart-aided near-
 capacity designs for wireless channels, 2nd edn. Wiley
32. Beh KC, Doufexi A, Armour S (2007) Performance evaluation of
 hybrid ARQ schemes of 3GPP LTE OFDMA system. In: IEEE
 18th International symposium on personal, indoor and mobile
 radio communications, pp 1–5
33. Nguyen D, Tran T, Nguyen T, Bose B (2009) Wireless broadcast
 using network coding. *IEEE Trans Veh Technol* 58(2):914–925

- 582 34. Ngo HA, Hanzo L (2014) Hybrid automatic-repeat-request 616
583 systems for cooperative wireless communications. *IEEE Commun* 617
584 *Surv Tutor* 16(1):25–45. First 618
- 585 35. IEEE standard for local and metropolitan area networks part 619
586 20: Air interface for mobile broadband wireless access sys- 620
587 tems supporting vehicular mobilityphysical and media access 621
588 control layer specification, IEEE Std 802.20-2008, pp 1–1039, 622
589 2008 623
- 590 36. IEEE standard for local and metropolitan area networks part 16: 624
591 Air interface for broadband wireless access systems amendment 625
592 3: Advanced air interface,” IEEE Std 802.16m-2011(Amendment 626
593 to IEEE Std 802.16-2009), pp 1–1112, 2011 627
- 594 37. IEEE standard for wireless man-advanced air interface for 628
595 broadband wireless access systems, IEEE Std 802.16.1-2012, pp 629
596 1–1090, 2012 630
- 597 38. Li JCF, Zhang W, Nosratinia A, Yuan J (2013) SHARP: spectrum 631
598 harvesting with ARQ retransmission and probing in cognitive 632
599 radio. *IEEE Trans Commun* 61(3):951–960 633
- 600 39. Hamza D, Aissa S (2014) Enhanced primary and secondary 634
601 performance through cognitive relaying and leveraging primary 635
602 feedback. *IEEE Trans Veh Technol* 63(5):2236–2247 636
- 603 40. Harsini JS, Zorzi M (2014) Transmission strategy design in 637
604 cognitive radio systems with primary ARQ control and QoS 638
605 provisioning. *IEEE Trans Commun* 62(6):1790–1802 639
- 606 41. Ao WC, Chen KC (2010) End-to-end HARQ in cognitive radio 640
607 networks. In: *IEEE Wireless communications and networking* 641
608 *conference (WCNC)*, pp 1–6 642
- 609 42. Touati S, Boujemaa H, Abed N (2013) Cooperative ARQ 643
610 protocols for underlay cognitive radio networks. In: *Proceedings* 644
611 *of the 21st European signal processing conference (EUSIPCO)*, 645
612 pp 1–5 646
- 613 43. Yue G, Wang X, Madhian M (2007) Design of anti-jamming 647
614 coding for cognitive radio. In: *IEEE Global telecommunications* 648
615 *conference 2007*, pp 4190–4194 649
44. Yue G, Wang X (2009) Design of efficient ARQ, schemes with 616
anti-jamming coding for cognitive radios. In: *IEEE Wireless* 617
communications and networking conference (WCNC), pp 1–6 618
45. Liu Y, Feng Z, Zhang P (2010) A novel ARQ, scheme based 619
on network coding theory in cognitive radio networks. In: *IEEE* 620
International conference on wireless information technology and 621
systems (ICWITS), pp 1–4 622
46. Liang W, Ng SX, Feng J, Hanzo L (2014) Pragmatic distributed 623
algorithm for spectral access in cooperative cognitive radio 624
networks. *IEEE Trans Commun* 62(4):1188–1200 625
47. Hu J, Yang LL, Hanzo L (2013) Maximum average service 626
rate and optimal queue scheduling of delay-constrained hybrid 627
cognitive radio in nakagami fading channels. *IEEE Trans Veh* 628
Technol 62(5):2220–2229 629
48. Makki B, Amat AGI, Eriksson T (2012) HARQ feedback in 630
spectrum sharing networks. *IEEE Commun Lett* 16(9):1337–1340 631
49. Makki B, Svensson T, Zorzi M (2015) Finite block-length analysis 632
of spectrum sharing networks using rate adaptation. *IEEE Trans* 633
Commun 63(8):2823–2835 634
50. Liang W, Nguyen HV, Ng SX, Hanzo L (2016) Adaptive-TTCM- 635
aided near-instantaneously adaptive dynamic network coding for 636
cooperative cognitive radio networks. *IEEE Trans Veh Technol* 637
65(3):1314–1325 638
51. Hong X, Wang J, Wang CX, Shi J (2014) Cognitive radio in 639
5g: a perspective on energy-spectral efficiency trade-off. *IEEE* 640
Commun Mag 52(7):46–53 641
52. Bertsekas D, Gallager R (1991) *Data networks*, 2nd edn. Prentice 642
Hall 643
53. Howard R (1971) *Dynamic probabilistic systems: Markov models*. 644
Wiley, New York 645
54. Ozcan G, Gursoy MC (2013) Throughput of cognitive radio 646
systems with finite blocklength codes. *IEEE J Selected Areas* 647
Commun 31(11):2541–2554 648
55. Lin S, Costello DJ Jr (1999) *Error control coding fundamentals* 649
and applications, 2nd edn. Prentice-Hall, NJ 650

Q5